World Conference on Timber Engineering Oslo 2023

EXPERIMENTAL STUDY ON CONTROL PARAMETERS FOR AUTOMATED APPLICATION AND IN- SITU PERFORMANCE ASSESSMENT OF JOINTS WITH SELF-TAPPING TIMBER SCREWS

Alexandra Eckert[1], Reinhard Brandner[2], David Glasner[3]

ABSTRACT: The paper in hand presents findings from experimental insertion tests with the purpose of establishing and quantifying necessary parameters for an automated application of the investigated self-tapping timber screws. The effects of input parameters such as contact force and revolutions per minute are examined and control parameters such as insertion moment and insertion length are recorded continuously. The biting-behaviour of screws is highly influenced by the contact force and the material parameters such as screw-diameter, screw-tip as well as the density and growth characteristics of the timber. With continuous control of insertion length and insertion moment a tight fit of the screw can be ensured, without damaging the screw or the surrounding timber. Given automatically applied screws with continuous recording of insertion moment and insertion length, the insertion energy can be calculated easily. As an in-situ performance assessment of automatically applied screws the hypothesis of estimating withdrawal characteristics on the basis of insertion energy is made. To validate this hypothesis, given experimental data of combined insertion and withdrawal tests is re-evaluated. A remarkable potential of predicting withdrawal properties with the insertion energy is found. This allows to thoroughly re-consider the design-to-execution process and the implementation of a research informed design process.

KEYWORDS: Automated application, insertion tests, withdrawal tests, self-tapping screws, in-situ performance assessment, research informed design

1 INTRODUCTION

The following studies were obtained as parts of the FFG BRIDGE project “CLT_joint” (project no. 883672), with the aim of developing an efficient, systematized and quality-assured connection solution for solid timber constructions with cross laminated timber (CLT). The solution is envisaged as a combination of timber-connection (application on CLT-components with self-tapping screws in course of joinery in the factory) and assembly-joint (joining of CLT-components on site). Due to the dominating quasi-brittle properties of timber components, it is intended that the timber-connection is designed with a sufficient over-strength to achieve the required ductility and energy dissipation specifically in the assembly-joint. Considering the prefabrication of the timber-connection this solution promises shorter assembly times and higher reliability and thus enhanced quality and cost-effectiveness in comparison to the current state of manually and completely on-site applied fasteners.

Known and already established, industrially implemented possibilities for an automated application of fasteners (e.g. automotive or aviation industry) motivate the integration of such processes supplemented by continuous quality control measures also within the timber industry, e.g. during the joinery of the CLT-elements. Required process steps for such, in the prefabrication integrated, application-units include separation, feeding and positioning, as well as the insertion of the screws and metal fittings. Common existing application units are limited to screws with small dimensions and correspondingly low max. insertion moments and primarily vertical insertion. For the expected screw dimensions used in timber construction (nominal diameter $d = 6$ to 12 mm, lengths up to 500 mm), the required flexibility to apply such screws at different angles (in and out of plane), together with higher insertion moments must be considered and necessary parameters for a controlled insertion need to be established.

Regarding performance-assessment, the hypothesis is made that the individual information on the insertion-energy, which can be calculated very easily assuming a continuous control of the insertion moment and insertion length, is more suitable for estimating the withdrawal capacity and the slip modulus than the information on the individual maximum insertion moment or the global product density (please note: density is currently the only timber-specific property for estimating the stiffnesses and strengths of fasteners anchored in timber in the course of the design). The background for the made hypothesis is that by recording the insertion energy, the interaction

[1] Alexandra Eckert, TU Graz, Institute of Timber Engineering and Wood Technology, Austria, alexandra.eckert@tugraz.at
[2] Reinhard Brandner, TU Graz, Institute of Timber Engineering and Wood Technology, Austria, reinhard.brandner@tugraz.at
[3] David Glasner, TU Graz, Institute of Timber Engineering and Wood Technology, Austria, david.glasner@tugraz.at

https://doi.org/10.52202/069179-0176

between the material and the fastener, influenced by local growth characteristics such as knots, is considered along the entire screw channel, whereas the single knowledge of the maximum insertion moment, although also considered as individual property, only represents a punctual information. The idea to estimate the withdrawal properties of self-tapping screws based on the insertion energy came up in frame of a previous research project, see [1]. A similar approach was already successfully applied for screws inserted in bones; see [2].

2 INSERTION TESTS

2.1 GENERAL INFORMATION

With the purpose of establishing and quantifying necessary control parameters, insertion tests were carried out. Special attention was set on the two critical phases of an automated insertion process: the biting of the screw-tip and the tightening of the screw-head.

2.2 MATERIALS AND METHODS

2.2.1 Materials and test overview

Insertion tests were carried out with self-tapping screws with countersunk heads, varying nominal diameters d = {8; 10; 12} mm, total lengths l = {180; 300; 400} mm and screw-tips {C; D; F; H}, see Figure 1 and Table 1.

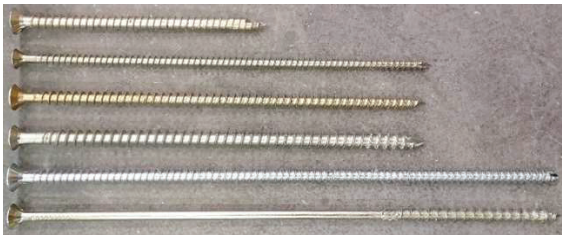

Figure 1: *Investigated self-tapping screws – from top to bottom: 10/180 mm with tip H, 8, 10, 12/300 mm with tip C, 10/400 mm with tip D and 10/400/120 mm with tip F.*

The screws were inserted in the middle layer of five-layer CLT-elements (layup 40 | 20 | 40 | 20 | 40 mm) made of Norway spruce (*Picea abies*). The angle between the axis of the screw and the fiber-orientation of the middle layer (short: load-grain angle α) varied between α = {0; 45; 90} °, see Table 1. In order to adequately represent the characteristics of timber used in construction practice, screws were also applied in finger joints, knots and other typical growth and product characteristics.

Table 1: *Matrix of investigated parameters, such as: screw-tip, nominal screw diameter d, screw length l and load-grain angle α.*

screw-tip	d [mm]			l [mm]	α [°]		
type H	–	10	–	180	0	45	90
type C	8	10	12	300	–	–	90
type D	–	10	–	400	0	45	90
type F	–	10	–	–	0	45	90

Twelve series (three series per screw-tip) with 20 replications each and thus a total of 240 screws were tested. The fully-threaded screws where inserted completely; partially-threaded screws with tip F were only tested in respect to their biting behaviour.

2.2.2 Test configuration

The insertion tests were carried out as illustrated in Figure 2. An electric drive on a fixed support drives the screw while a standard pneumatic cylinder applies pressure between the timber specimen on the moving support and the screw. Both, revolutions per minute (RPM) of the electric drive and contact pressure of the standard pneumatic cylinder, are controlled manually. A cable extensometer between the fixed and the moving support is measuring the displacement. The insertion moment is recorded by a torque transducer, which is placed between the screw and the electric drive. In order to measure the screw force (force between wood specimen and screw head while tightening the screw) a load cell is placed between two steel plates in front of the timber specimen, mirroring a steel-timber joint with outer steel plate. The inserted length of the screws is reduced by 80 mm (height of the load cell plus thickness of steel plates). During insertion testing the parameters time (t), insertion length (l_i)*, insertion moment (M), rotation angle (φ) and screw force (F) were recorded continuously (measurement rate 5 Hz).

* possible small angular deviations might cause differences between insertion length and measured displacement; these are neglected

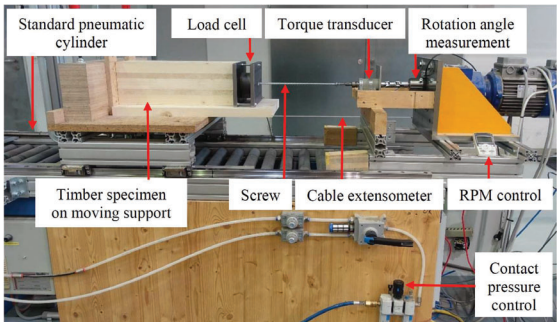

Figure 2: *Test setup and measuring devices of insertion tests.*

2.2.3 Input parameters

To determine optimal conditions for rapid biting of the screw, the effects of input parameters, such as revolutions per minute (RPM) and contact force (CF) between the wood specimen and the application device were investigated. The input parameters RPM and CF were chosen with {50; 100} Hz and by setting the contact pressure to {0.5*; 1.0; 2.0; 4.0; 6.0} bar, respectively. After a small test series and by using the load cell, the according results of the CF are {0.11; 0.14; 0.29; 0.61; 0.95} kN. These results are lower than the calculated force of the standard pneumatic cylinder (contact pressure times cylinder area), which attributes to frictional loss.

* due to inaccuracy of the pressure-control in the lower range the value 0.5 is assumed to be approx. 0.7 bar (corresponds with resulting CF)

https://doi.org/10.52202/069179-0176

2.2.4 Test procedure

The recording of said parameters started after placing the screw tip through the load cell onto the timber specimen. CP and RPM started simultaneously. While the set CP was reached immediately, the acceleration of RPM took a view seconds to reach its set value.

Special attention was set on the critical phase of the insertion: the biting of the screw-tip. In case of no biting after 20 revolutions, the biting process was considered as failed and the CP was raised until biting occurred which enabled the continuation of the insertion test. After reaching a specific insertion length during the insertion (depending on the pitch of the screw and the set RPM), the RPM was decelerated to 5 Hz for better observation of the other critical phase: the tightening of the screw. The testing finished after failure due to torsion of the screw or overturning of the screw.

2.2.5 Evaluation of biting behaviour

To evaluate the biting behavior, the continuous recording of insertion length (l_i), rotation angle (φ) and insertion moment (M) was examined. The biting behaviour was assesed with the amount of revolutions until the screw-tip bite. The evaluation is limited to 20 revolutions, because during testing at this point the biting was classified as failed. When biting occurred the gradient of the insertion length-revolution graph corresponded with the respective pitch (p) of the screw and the insertion moment increased, as exemplarily illustrated in Figure 3.

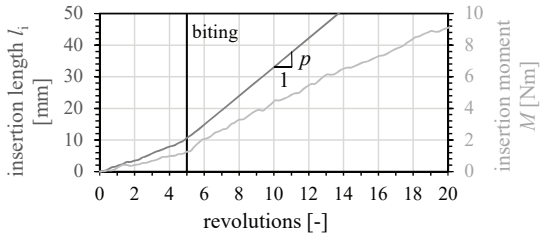

Figure 3: *Example of biting evaluation on insertion length (l_i) and insertion moment (M) plotted over revolutions.*

2.3 RESULTS AND DISCUSSIONS

2.3.1 Density and moisture content

There is only a slight variability in the density between the series and the ranges are quite comparable. The average density ($\rho_{12,mean}$) is 461 kg/m³ with a range from 408 to 515 kg/m³ (CV = 4.7 %). The average wood moisture content is 11.7 %. Further details can be found in the accompanying test report, see [3].

2.3.2 Biting behaviour

To investigate the influence of parameters on the biting behaviour, different sets of test data with equal boundary conditions are compared. Figure 4 shows different load-grain angles and contact forces with equal boundary conditions d = 10 mm and screw tips H, D and F. Wood specimens with knots or other growth or product characteristics are excluded in this diagram to concentrate on the influence of α. The results only differ noticeably in the low CF-range for α = 0°. In the higher range of CF, the influence of the load-grain angle seems to diminish.

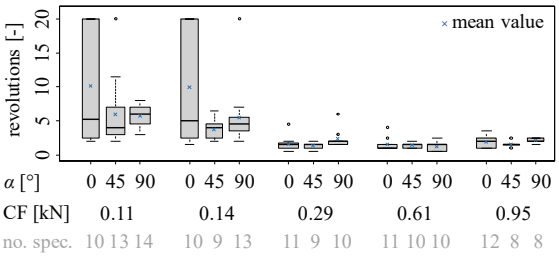

Figure 4: *Biting behaviour vs. load-grain angle α and contact force CF (please note: statistical values of groups exceeding the evaluation-limit of 20 revolutions represent lower estimates).*

In Figure 5 the biting behaviour is shown for different screw diameters and contact forces with equal boundary conditions α = 90° and screw-tip C. In this diagram data from screw insertion in knots and other growth and product characteristics are included. The influence of the screw diameter on the biting-behaviour is evident, but an overall more perceivable effect is again reached by the CF. Setting the CF to approx. 0.3 kN already achieved successful biting for those tested boundary conditions.

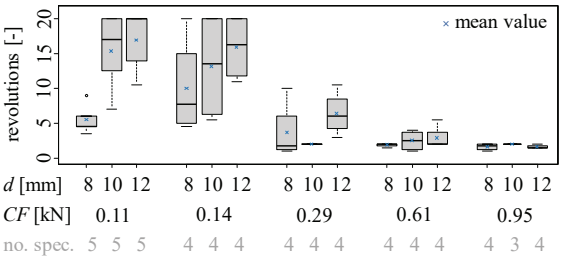

Figure 5: *Biting behaviour vs. diameters d and contact force.*

The required CF for a rapid biting in knots is shown in Figure 6, representing the collected data of screw tips inserted in knots with d = 10 mm regardless of the type of the screw tip {H; C; D; F} and α = {0; 45; 90}°.

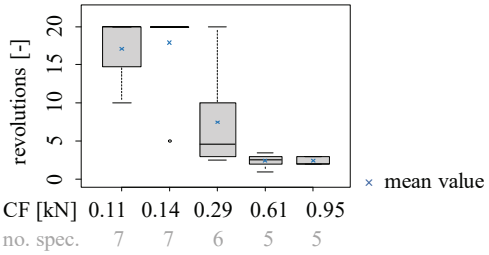

Figure 6: *Biting behaviour of screws applied in knots.*

Regarding RPM no influence on the biting behaviour can be detected due to the fact that the biting often took place

https://doi.org/10.52202/069179-0176

before the set RPM was reached. Yet the observation was made, that in cases of no biting after 20 revolutions where the RPM had reached its set value, the CF needed to be increased even higher at RPM = 100 Hz than at 50 Hz to achieve biting.

2.3.3 Tightening – insertion moment

Beside the biting of the screw, the tightening of the screw represents another critical phase within an automated insertion process. Figure 7 plots the insertion moment of screws with different diameters (d) and the following boundary conditions: $\alpha = 90$ °, $l_i = 220$ mm and screw tip C. The lower box-plots represent the distribution of the max. insertion moment measured from the screw-tip to the beginning of the screw-head and the highest plots represent the max. insertion moment measured from contact of the screw head with the sinking until failure. The full dots in between represent the characteristic values of the torque resistance ($f_{tor,k}$) for each screw diameter according to the European Technical Assessments (ETAs) of these screws. The insertion moment increases with increasing screw diameter, considering the data until head and incl. head.
The max. insertion moment incl. head exceeds the torque resistance by a significant margin. Although the actual resistance of the tested screws is probably higher than the characteristic value, the amount of deviation is most likely a result of the interaction between screw head and steel plate (please note: screws compared in Figure 7 have the same underhead milling ribs).

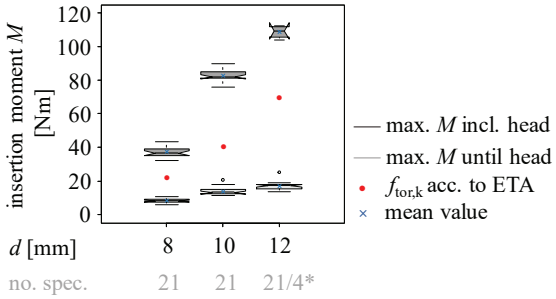

Figure 7: *Diameter vs. max. insertion moment until the beginning of the screw head and max. insertion moment incl. embedment and tightening of the screw head in the sinking of the steel plate (* only 4/21 screws with d = 12 mm failed by torque as the screw drive reached their max. capacity before).*

Figure 8 plots the insertion moment of screws with different insertion lengths and the following boundary conditions: $d = 10$ mm and $\alpha = 90$ °. Whereas screws with $l_i = 100$ and 220 mm had similar underhead milling ribs, screws with $l_i = 320$ mm had a smooth underhead surface. The max. insertion moment until head (lower boxplots) increases with increasing insertion length.
The results of the max. insertion moment incl. head (higher boxplots) of screws with milling ribs ($l_i = 100$ and 220 mm) also increase with increasing insertion length. Between the heads of these screws and the sinkings a high interaction was observed in form of abrasion of the sinking, which is attributed to friction and milling. The investigated screws with a smooth underhead surface ($l_i = 320$ mm) are not reflecting the same effect. This is most likely due to the lower interaction between the head and the sinking which in this case can be attributed solely to friction. Nonetheless, their data incl. head exceeds $f_{tor,k}$ according to the ETA (full dot) by a significant margin.
Screws with insertion lengths $l_i = \{220; 320\}$ mm failed due to torsion of the screw. The screws with the lowest insertion length failed due to overturning of the screw. In combination with a relatively high $f_{tor,k}$ this leads to an overlap of the data incl. head and $f_{tor,k}$ (please note that 10 d represents a low insertion length in timber constructions where high load bearing screwed joints are often designed for screw tension failure).
Speaking for the critical phase of screw tightening, for screws designed for tension failure (where the possibility of overturning principally can be neglected) higher tightening moments are possible and also often required compared to standard screw torsion tests.

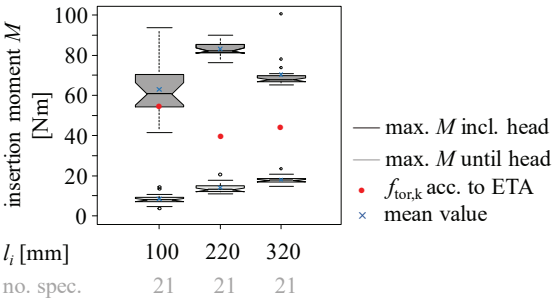

Figure 8: *Insertion length vs. max. insertion moment until the beginning of the screw head and max. insertion moment incl. embedment and tightening of the screw head in the sinking of the steel plate.*

2.3.4 Further results

The insertion energy was calculated with the pitch of the screw and the insertion moment in combination with the insertion length according to Equation (1) in Chapter 3.2. Results show an increase in insertion energy with increasing nominal screw diameter. The same effect is observed, when analysing the maximum screw force of the tested diameters.
The insertion energy and the maximum screw force also increase with increasing insertion lengths, although this effect is limited by the screw capacity itself; the tensile strength ($f_{tens,k}$).
When analysing the influence of input parameters CF and RPM on the maximum insertion moment, the insertion energy and the screw force, no correlation can be determined. For further details see [3].

https://doi.org/10.52202/069179-0176

3 PERFORMANCE-ASSESSMENT AND OPTIONS FOR RESEARCH INFORMED DESIGN (RID)

3.1 SETTING UP THE HYPOTHESIS AND GENERAL COMMENTS

In the following, the hypothesis is analysed, that the total insertion energy, determined along the total insertion length, serves as a better, more reliable predictor for the withdrawal properties (strength and slip modulus) than the maximum insertion moment, as one punctual characteristic, and the density, whether it is available as local or global (product) characteristic.

The background to this consideration is simply the fact, that the total insertion energy, as integral of the measured insertion energy along the insertion length, takes local irregularities into account, such as knots, checks and reaction wood. The prerequisite for this is a quasi-continuous recording and data processing of insertion moment and insertion length together with parameters of thread geometry, as it would be possible during an automated and controlled application of screws. Saying that, the insertion energy provides additional information on screw application but cannot substitute others, e.g. the insertion moment, which still needs to be controlled to prevent overturning and torque failure of the screw.

The following sections analyse the hypothesis in detail. As this is done as a second, widely independent part of the overall paper, the principle structure of a research paper is widely repeated.

3.2 MATERIALS AND METHODS

In total 284 data sets from twelve series, each with 20 to 24 specimens, from insertion tests without predrilling acc. to [5] and withdrawal tests acc. to [6] conducted on the same specimens are used. The tests, made in Norway spruce (*Picea abies*), comprised three different density classes {A; B; C}, two different screw types {RF; P1}, each with a nominal diameter d = 8 mm, and two different load-grain angles $\alpha = \{0°; 90°\}$. Series of the same density class were organised as matched samples, i.e. as series with similar density distributions. To test solely the thread, all screws were screwed through the specimens with a nominal thickness in loading direction of 50 mm, so that the tip and compressor left the opposite side. This boundary condition should be kept in mind as it represents a rather uncommon practical condition. The specimens were conditioned at 20 °C and 65 % rel. humidity before testing. Details on the determination of the moisture content u [%], the local density ρ_{12} [kg/m³], the insertion moment M [Nm], the withdrawal strength f_{ax} [MPa] and the slip modulus K_{ser} [kN/mm] are provided in [3] and [4]. The insertion tests were re-evaluated to determine not only the maximum insertion moment but also the insertion energy W [Nm] calculated acc. to Equation (1):

$$W = \frac{2\pi}{p} \int M \, \partial l_i \qquad (1)$$

where l_i is the insertion length [mm] and p the pitch of the screw [mm].

Three different conditions were investigated for the completion of the summation: (1) the final insertion length, (2) the point of the maximum insertion moment, and (3) 50 mm insertion length. In the following, the insertion energy acc. to (3) is used as it is the most representative for practical applications; it is also rather close to (2); see [3].

3.3 RESULTS AND DISCUSSIONS

3.3.1 General statistics and regression analyses

Table 2 summarizes the main statistics per test series for the most important properties. Statistics for the moisture content are provided in [3] (average moisture contents per series within 12.5 and 13.2 %).

The average densities confirm the successful creation of matched samples within each density class and clearly different densities between the classes. The total bandwidth of 330 to 620 kg/m³ covers a typical range for Norway spruce. The maximum insertion moments for P1 are on average slightly higher than for RF. The difference between both screw types is even higher for the slip modulus, irrespective of the load-grain angle. In contrast, the withdrawal strengths are similar at 90° and slightly lower for P1 at 0°, due to the thicker core of P1; see [7]. Compared to P1, for RF the average values for the insertion energy are in trend clearly higher in case of $\alpha = 0°$ and slightly lower in case of $\alpha = 90°$. The coefficients of variation (CV) for the insertion energy are widely within 15 and 20 % and similar as for M; see [3].

***Table 2**: Main statistics of analysed series of insertion and withdrawal tests.*

Series	n [–]	$\rho_{12,mean}$ [kg/m³]	$f_{ax,mean}$ [MPa]	$K_{ser,mean}$ [kN/mm]	M_{mean} [Nm]	W_{mean} [Nm] | CV [%]
A_P10	24	362	4.5	23.0	2.9	139 | 17
A_RF0	24	358	4.9	18.0	2.8	150 | 10
A_P190	24	368	5.0	13.1	3.2	160 | 12
A_RF90	24	373	5.1	11.3	2.8	155 | 17
B_P10	24	442	3.9	21.3	3.4	163 | 8
B_RF0	24	441	4.4	18.3	3.3	181 | 10
B_P190	23	448	6.3	16.1	4.6	218 | 11
B_RF90	24	450	6.2	14.3	4.0	210 | 13
C_P10	24	536	5.6	30.8	4.9	237 | 25
C_RF0	24	539	6.4	26.4	4.8	265 | 22
C_P190	21	539	7.7	22.5	6.1	290 | 17
C_RF90	24	543	7.8	18.1	5.4	286 | 18

For the statistical analyses of the relationships between the withdrawal properties $\boldsymbol{Y} = \{f_{ax}; K_{ser}\}$ and the indicating properties $\boldsymbol{X} = \{\rho_{12}; W\}$ power regression models are applied which consequence from assumed lognormal variables; see Equation (2):

$$Y_j = \beta_0 X_j^{\beta_1} \varepsilon_j \quad \Leftrightarrow \quad \ln(Y_j) = \ln(\beta_0) + \beta_1 \ln(X_j) + \varepsilon_j \qquad (2)$$

where $\{\beta_0; \beta_1\}$ are the regression coefficients and ε is the standard error. Regression models are calculated for each

https://doi.org/10.52202/069179-0176

screw type {RF; P1} and load-grain angle α = {0°; 90°} whereby the density groups {A; B; C} are combined. The outcomes for the estimated regression coefficients, standard errors (s_e) and adjusted coefficients of determination (r^2_{adj}) are summarized in Table 3.

***Table 3**: Regression coefficients and main statistics of power regression models per screw type and load-grain angle.*

Group	Model	$\hat{\beta}_0$	$\hat{\beta}_1$	s_e	r^2_{adj}
RF0	$f_{ax} \sim \rho_{12}$	0.062	0.724	0.225	0.23
	$f_{ax} \sim W$	0.138	0.686	0.176	0.53
	$K_{ser} \sim \rho_{12}$	49.77	0.990	0.179	0.48
	$K_{ser} \sim W$	366.9	0.763	0.133	0.71
RF90	$f_{ax} \sim \rho_{12}$	0.005	1.164	0.071	0.88
	$f_{ax} \sim W$	0.216	0.631	0.081	0.84
	$K_{ser} \sim \rho_{12}$	5.885	1.275	0.123	0.74
	$K_{ser} \sim W$	365.7	0.685	0.133	0.70
P10	$f_{ax} \sim \rho_{12}$	0.063	0.702	0.225	0.21
	$f_{ax} \sim W$	0.140	0.673	0.172	0.54
	$K_{ser} \sim \rho_{12}$	194.6	0.793	0.216	0.27
	$K_{ser} \sim W$	837.1	0.653	0.178	0.50
P190	$f_{ax} \sim \rho_{12}$	0.004	1.200	0.093	0.82
	$f_{ax} \sim W$	0.112	0.750	0.080	0.87
	$K_{ser} \sim \rho_{12}$	2.557	1.441	0.138	0.75
	$K_{ser} \sim W$	145.8	0.883	0.135	0.76

These power regression analyses are illustrated exemplarily for the screw type RF and α = 0° in Figure 9 and Figure 11 and for α = 90° in Figure 10 and Figure 12.

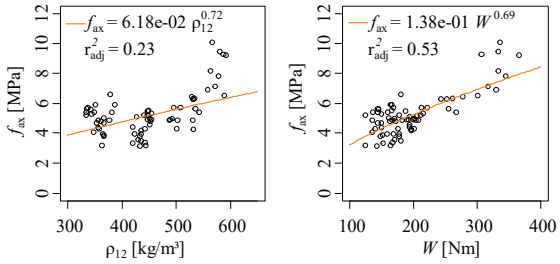

***Figure 9:** Power regression analysis for f_{ax} vs. ρ_{12} (left) and f_{ax} vs. W (right) exemplarily for RF and α = 0°.*

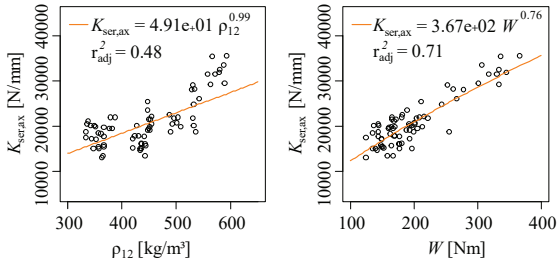

***Figure 10:** Power regression analysis for $K_{ser,ax}$ vs. ρ_{12} (left) and $K_{ser,ax}$ vs. W (right) exemplarily for RF and α = 0°.*

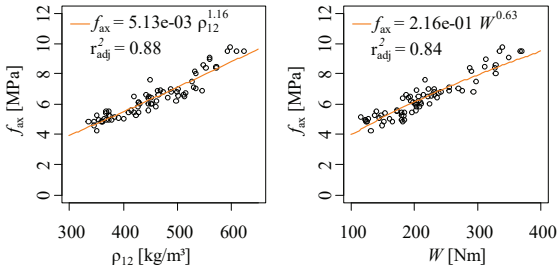

***Figure 11:** Power regression analysis for f_{ax} vs. ρ_{12} (left) and f_{ax} vs. W (right) exemplarily for RF and α = 90°.*

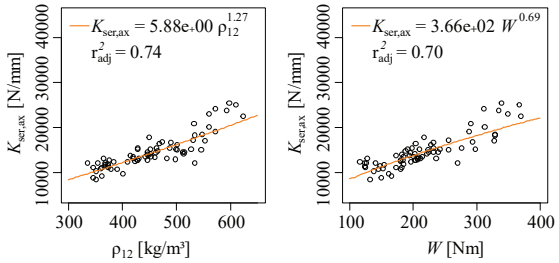

***Figure 12:** Power regression analysis for $K_{ser,ax}$ vs. ρ_{12} (left) and $K_{ser,ax}$ vs. W (right) exemplarily for RF and α = 90°.*

With ρ_{12} as indicating property, the regression coefficients for α = {0°; 90°} are clearly different whereas in case of W the coefficients are rather close. The values for r^2_{adj} confirm previous findings of the very limited capability of ρ_{12} to predict withdrawal properties at α = 0°; see [8] and [9]. This circumstance is usually of less importance as the reference properties normally refer to α = 90° and properties at deviating conditions are adapted accordingly by means of corresponding relationships. W is rather able to reliably predict the withdrawal properties which is clearly demonstrated by overall higher degrees of determination. The total insertion energy also adapts more individually to the insertion conditions which is also visible in Figure 9 to Figure 12 where for the same withdrawal data the ratio $\rho_{12,max}$ / $\rho_{12,min}$ is approximately two whereas it is four for W_{max} / W_{min}. To conclude: based on this analysis there is a clear indication that the total insertion energy serves overall as better and more reliable predictor of the withdrawal strength and slip modulus than the local density.

In order to benefit accordingly from this finding, the acquisition of the data required for this in the course of an automated, controlled screw application process is indispensable. It should be mentioned that the insertion energy is influenced by certain screw features (e.g. cutters and compactors, tip geometry, slide coating, screw length in the case of partially-threaded screws, etc.) which do not (or only to a minor extent) affect f_{ax}. As a result, more general models to describe f_{ax} by means of the insertion energy might need to consider these parameters and thus the individual screw type. In the following it is assumed that this will take place.

3.3.2 Analysis of the current design process and the potential benefits of the new findings

Within the current design process and with focus on the resistance part, the engineer doing the design usually follows design standards and applies characteristic properties, which are tabulated in referenced product standards or can be easily calculated from standardized relationships. The standardized characteristic properties and relationships need to account for all the uncertainties associated with the assumed product, strength class, production, producer and execution; see e.g. [10]. As long as the structure is not realised, these uncertainties belong to the aleatoric part; only the timber product and the nominal strength class are determined by the designer who assumes that it will also be executed that way. By erecting the structure, the aleatoric part becomes epistemic; the properties are fixed but usually still remain unknown.

In the current design of joints in timber, the properties of fasteners determined from their interaction with timber are only related to one timber property, the characteristic (5 %-quantile) of the density of the specific timber product and the nominal strength class. This value has to be distinguished from the local density which is usually determined in tests and used as indicating property in regression analyses to derive the before mentioned standardized relationships. The product density itself is usually not representative for the individual fastener properties as homogenisation effects, caused by the composition of products out of components (e.g. glulam composed of laminations) are considered in setting the characteristic values, whereas fasteners often penetrate only one or a limited number of components and therefore do not realize the same homogenisation effects ([11], [12]).

An automated controlled screw application system combined with the possibility to receive direct information on the local insertion properties, a set of models for a reliable estimation of the individual fastener withdrawal properties and newly created opportunities to adapt the joint execution, e.g. by adaptation of the insertion length, the number of fasteners within a joint and/or the spacing between joints in discretely equipped connection lines, provides a set of new possibilities to thoroughly re-consider the design-to-execution process by implementing research informed design (RID; see [13]). In doing so, a number of uncertainties inherently associated with the current design process would be eliminated. Designers could compensate this by setting higher characteristic properties, referring to higher quantile values, and/or by lower partial safety factors. During the automated screw and joint application, the fulfilment of the requirements set by the designer is individually controlled and adapted if necessary. This way, the determined but in current design-to-execution processes usually remaining unknown properties become known to a significant extend. Thereby, the model uncertainties associated with the estimated withdrawal properties and all uncertainties associated with the execution and quality assurance process, including the uncertainty associated with the measurement itself, shall be considered, e.g. by using lower quantile values of the estimates. For example, under the made assumption of lognormal variables the regression models in Table 3, which lead to average estimates for Y_j given a specific value of X_j, could be easily transformed to calculate quantile values, e.g. acc. to Equation (3):

$$y_{p,j} = \exp\left(\left(\ln(\beta_0) + \beta_1 \ln\left(X_j\right)\right) + z_p \sigma_{\ln(Y_j)}\right) \qquad (3)$$

where $y_{p,j}$ is the p-quantile value of Y for the j-th screw, z_p is the p-quantile value of the standard normal distribution and $\sigma_{\ln(Y_j)}$ is the standard deviation of Y for the j-th screw in the logarithmic domain.

The benefit of this approach is exemplarily demonstrated for the series C_RF90. The reason for selecting this series is its representativeness in respect to CV[f_{ax}] = 14.6 % and CV[ρ_{12}] = 7.0 %; see e.g. [7], [8], [14]. Please note: this demonstration is not intended to validate any of previously presented models. To ensure equal conditions for the following comparisons, all statistics and models are taken directly from series C_RF90.

The characteristic values for the density and the withdrawal strength, as 5 %-quantiles of assumed lognormal variables, are $\rho_{12,05}$ = 484 kg/m³ and $f_{ax,05}$ = 6.1 MPa, respectively. Following the current version of prEN 1995-1-1 [15] and [14], the characteristic withdrawal strength for a material featuring a similar characteristic density as series C_RF90 would be $f_{ax,k}$ = 5.9 MPa. By considering that $f_{ax,k}$ acc. to [15] has to account for all the additional uncertainties related to product, batch and many more (see e.g. [10]), the values appear as too close in this case.

The power regression model $f_{ax} \sim W$ for series C_RF90 reads $f_{ax,j} = 0.1075 \cdot W_j^{0.7583}$, with $r^2 = 0.89$, so 89 % of the variance in f_{ax} can be explained by the regression model; thus, only 11 % uncertainty remain in the individually estimated $f_{ax,j}$. To be in line with current design procedures, by means of Equation (3) 5 %-quantile values $f_{ax,j,05}$ are calculated for each individually estimated $f_{ax,j} \mid W_j$. The average value of these 5 %-quantiles is $f_{ax,j,05,mean}$ = 6.63 MPa. By considering the individual potentials, in comparison to $f_{ax,05}$ for series C_RF90 and $f_{ax,k}$ acc. to [15], the characteristic value is on average 9 % and 13 % higher, respectively. The bandwidth of the ratio $f_{ax,j,05,est} / f_{ax,j,test}$ is 0.77 to 0.92, the average value 0.85, which means that the applied approach is conservative; theoretically the capacity of 1 / 24 specimens could be overestimated.

Acc. to the load and resistance factor design (LRFD) approach, as implemented in the Eurocode, the reduced uncertainty not only consequence in higher characteristic values but also in lower partial safety factors γ_M. Acc. to [16], for simple cases and lognormal variables the design value can be calculated acc. to Equation (4):

$$y_d = \mu_Y \exp\left(-\frac{1}{2}\ln(1 + CV_Y^2) - \alpha_s \beta \sqrt{\ln(1 + CV_Y^2)}\right) \qquad (4)$$

https://doi.org/10.52202/069179-0176

where α_s is the sensitivity factor and β the target reliability index. In the following a 50-year reference period with $\alpha_s = 0.8$ and $\beta = 3.8$ for buildings in consequence class CC2 are applied. Acc. to [15] the reference partial safety factor for connections is $\gamma_M = 1.30$. Considering the significantly reduced uncertainty associated with the individually estimated withdrawal strengths $f_{ax,j}$, the partial safety factor can be adapted accordingly by reformulating Equation (4). In this special and simplified case $\gamma_M = 1.05$ would be sufficient to reach the same reliability (please note: $\gamma_M = 1.30$ is already higher than required for the reference case with $CV[f_{ax}] = 15$ %).
Although this demonstration example is rather simplified and could be also further elaborated by means of a Baysian approach, it clearly shows the advantages of RID in the sense of applying regression equations with high prediction quality for an individual estimation of withdrawal properties by means of in-situ acquisition of indicating properties. The reduced uncertainty allows to apply higher characteristic values and lower partial safety factors. Apart from that, knowing more about the individual screw properties in combination with a controlled screw application also raises the knowledge on the group behaviour. This enables to increase the effective number of screws accountable in the design, i.e. to apply a higher n_{ef}.

4 CONCLUSIONS

Within this contribution the potentials of an automated and controlled screw application are exemplarily analysed. The first part discusses the basic setting, parameters and requirements to secure a controlled automated screw application for the investigated screws. The second part outlines the power of the insertion energy as indicator for the withdrawal properties and demonstrates exemplarily the advantages of an individual estimation of the screw properties instead of using characteristic values of the population as common in the current design. In the following, the main conclusions of both parts are given.

4.1 AUTOMATED APPLICATION – CONTROL PARAMETERS

The automated application process is divided into its phases: (feeding and) positioning, biting, insertion and tightening (see Figure 13).
In the following paragraphs the established control parameters and their influences are summarized for each application phase. Furthermore, quantified suggestions for an automated application of the investigated self-tapping screws with countersunk heads connecting steel components with timber specimens of a typical density according to Norway spruce, diameters of $d = \{8; 10; 12\}$ mm and insertion lengths designed for screw tension failure, are made.

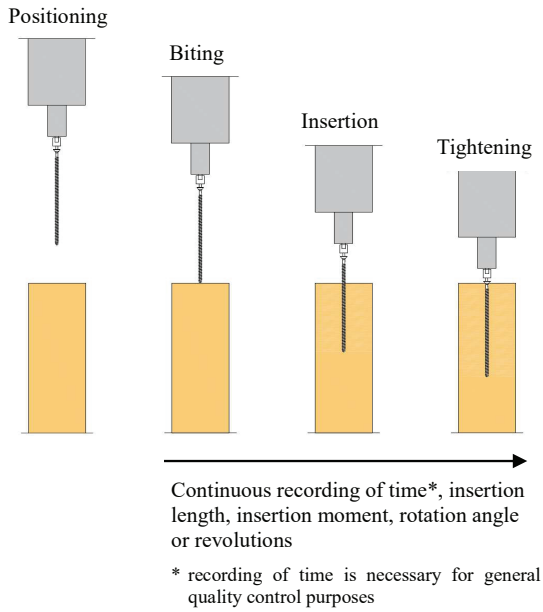

Figure 13: *Principle phases of an automated screw application process.*

- For feeding and positioning information on the screw (type, diameter, length and head), the screw drive, the application angles (in and out of plane) and position on the timber specimen are necessary.
- Strong influences on the biting behavior can be traced back on the contact pressure, the screw characteristics (diameter, tip-type) and on the local properties of the anchoring timber (e.g. density, growth characteristics). Overall, the load-grain angle α was found to have only a minor influence, althought the test results show that biting of screws inserted in grain ($\alpha = 0°$) is slightly more difficult than at $\alpha = 45°$ or 90°. Knowledge of the above mentioned boundary conditions is necessary to define a sufficient contact pressure. In general, a higher contact force is required for larger screw diameters and/or higher densities (including growth characteristics). Within the tested boundary conditions a contact force between 0.5 and 1.0 kN is suggested for rapid biting. The upper limit is set to prevent bending of the screw and damage of the timber specimen in the area of the tip. It is suggested to set the RPM to approx. 20 Hz for rapid biting of the screw.
- As for the insertion of the thread, control of the insertion length and the insertion moment is necessary to prevent failure due to torsion. RPM can be accelerated after biting. To prevent the screw from overturning a limitation of the insertion moment of 70 % of the respective torque resistance is advised.
  Before the tightening of the screw the RPM has to be decelerated in time at a certain insertion length, depending on the pitch of the screw, the RPM during insertion and the deceleration rate of the RPM. Furthermore, angular deviations of the screw must be

taken in account when setting the insertion length for deceleration.

- It is advised to decelerate the RPM asymptotically to 5 Hz (or less) to tighten the screw in a controlled manner, as the insertion moment increases very rapidly when the screw head contacts the sinking. To achieve a tight fit of the screw without failure, limiting the tightening torque with 80-90 % of the torque resistance (depending on underhead features) is advised.

4.2 IN-SITU PERFORMANCE ASSESSMENT – INSERTION ENERGY

- The insertion energy, which can be measured continuously in the course of a controlled automated screw application, has been identified as an extremely powerful predictor for the withdrawal properties of the investigated screw types.
- The high degrees of determination of presented power regression models $f_{ax} \sim W$ and $K_{ser} \sim W$ based on the investigated data sets demonstrate exemplarily the possibility for a significant reduction of the uncertainty in individually estimated withdrawal properties. As consequence, on average higher characteristic withdrawal properties and overall lower partial safety factors for the controlled failure modes could be applied.
- Overall better controlled and research informed executed joints might also be designed for higher capacities which is in addition supported by a higher accountable effective number of fasteners (n_{ef}) for the controlled failure modes. In order to react appropriately on differences between designed and in-situ estimated withdrawal properties, opportunities to adapt the joint execution are required, e.g. by adaptation of the insertion length, the number of fasteners within a joint and/or the spacing between joints in discretely equipped connection lines. This together provides a set of new possibilities to thoroughly re-consider the design-to-execution process by implementing research informed design (RID).
- This new process would have positive effects not only on the overall efficiency of prefabricated timber constructions but in particular on the over-strength-design for the brittle failing connection components since the existing potential could be better exploited. The resulting lower ratio between the properties of ductile and brittle failure mechanisms consequently would yield an economically more viable solution in particular for the design in case of characteristic load scenarios.
- Nevertheless, it needs to be considered that the investigations on the total insertion energy to date are limited to Norway spruce, screw types {RF; P1}, nominal screw diameter $d = 8$ mm, insertion length 50 mm, self-tapping insertion, load-grain angles $\alpha = \{0°; 90°\}$ and screwing through the specimen. Additional investigations are needed to further validate the applicability of the presented approach, in particular under variation of the nominal screw diameter, insertion length, additional load-grain angles and without screwing through the specimen. In addition, certain parameters need to be considered which have an effect on the insertion energy but not on the withdrawal properties. Consequently, structural reliability investigations need to be intensified for a fundamental quantification of expectable gains.

ACKNOWLEDGEMENT

The publication was written in frame of the research project FFG BRIDGE 1 “CLT_joint” (no. 883672) and received public funding by the Austrian Research Promotion Agency (FFG). Their support and the support by the commercial partners, Schmid Schrauben Hainfeld GmbH (Hainfeld, Austria) and TechnoWood AG (Alt St. Johann, Switzerland) are thankfully acknowledged.

REFERENCES

[1] Glasner D., Ringhofer A., Braun W., Hubmann G.: Energy demand for the driving in of self-tapping timber screws and its applicability. WTCE’23, Oslo, Norway, 2023.

[2] Gilmer B., Lang S.: Dual Motor Drill Continuously Measures Drilling Energy to Calculate Bone Density and Screw Pull-out Force in Real Time. *Wolters Kluwer Health, Inc.*, California, USA, 2018.

[3] Eckert A., Brandner R.: Anbisstests und Eindrehversuche im Rahmen des Arbeitspaketes 5 – MOUNT. *Research Report*, Graz University of Technology, Graz, Austria, 2022 (in German).

[4] Reichinger T.: Ausgewählte Untersuchungen zum Tragverhalten einer für Hartlaubholz optimierten Holzbauschraube (in German). *Master Thesis*, Graz University of Technology, 2017.

[5] EN 15737 Timber Structures – Test methods – Torsional resistance of driving in screws. CEN, 2009.

[6] EN 1382 Timber structures – Test methods – Withdrawal capacity of timber fasteners. CEN, 1999.

[7] Brandner R., Ringhofer A., Reichinger T.: Performance of Axially-Loaded Self-Tapping Screws in Hardwood: Properties and Design. *Engineering Structures*, 188:677–699, 2019.

[8] Ringhofer A., Brandner R., Schickhofer G.: A Universal Approach for Withdrawal Properties of Self-Tapping Screws in Solid Timber and Laminated Timber Products. INTER/48-7-1, Sibenik, Croatia, 2015.

[9] Brandner R., Ringhofer A., Grabner M.: Probabilistic Models for the Withdrawal Behavior of Single Self-Tapping Screws in the Narrow Face of Cross Laminated Timber (CLT). *European Journal of Wood and Wood Products*, 76(1):13–30, 2017.

[10] Fink G., Kohler J., Brandner R.: Application of European design principles to cross laminated timber. *Engineering Structures*, 171:934–943, 2018.

[11] Ringhofer A., Brandner R., Schickhofer G.: Withdrawal resistance of self-tapping screws in unidirectional and orthogonal layered timber

https://doi.org/10.52202/069179-0176

products. *Materials and Structures*, 48(5):1435–1447, 2015.
[12] Brandner R., Bratulic K., Ringhofer A.: Serial Correlation of Withdrawal Properties from Axially-Loaded Self-Tapping Screws. ICASP12, Vancouver, Canada, 2015.
[13] Peavey E., Vander Wyst K.B.: Evidence-Based Design and Research-Informed Design: What's the Difference? Conceptual Definitions and Comparative Analysis. *HERD: Health Environments Research & Design Journal*, 10(5):143–156, 2017.
[14] Westermayr M., Brandner R., Ringhofer A., Mahlknecht U., van de Kuilen J.W.G.: Performance, design and execution of screwed steel-timber end-grain connections. INTER/55-7-2, Bad Aibling, Germany.
[15] prEN 1995-1-1: Eurocode 5 Design of timber structures – Part 1-1: General rules and rules for buildings. CEN, 2022.
[16] prEN 1990: Eurocode 0: Basis of structural design. CEN, 2022.